JOURNAL OF MATERIALS 16 (1981) 397–406

Steady-state creep in a 25 wt % Cr–20 wt % Ni austenitic stainless steel

Y. TAKAHASHI, T. YAMANE
Department of Materials Science and Engineering, Osaka University, Suita 565, Japan

Steady-state creep behaviour of a 25 wt % Cr–20 wt % Ni stainless steel without precipitates was studied in the stress range 9.8 to 39.2 MPa at temperatures between 1133 and 1193 K. The results of stress-drop tests indicate that, in the steady-state creep region, diffusion-controlled recovery creep is dominant. Such recovery creep can be accounted for in terms of the composition of the internal stress, $\sigma_i = \sigma_s + \sigma_c$, except in the case of fine-grained specimens where $d < 80\,\mu$m, where d is the mean grain diameter, σ_s is possible to reduce easily and is comparable to the driving stress for creep, and σ_c is the persistent stress field due to metastable substructure. In the fine-grained specimens, it is suggested that the steady-state creep is dominantly controlled by grain boundaries.

1. Introduction

High-temperature dislocation-creep models of crystalline solids can be classified into those of thermally activated creep and those of diffusion-controlled recovery creep [1, 2].

In the thermally activated creep model, localized short-range obstacles are superposed on a periodic internal stress field which is attributed to long-range obstacles. Because thermal agitation can directly help in overcoming the short-range obstacles, even if the applied stress is reduced a little, the creep deformation can still proceed. As a result the applied stress is divided into two components, i.e. thermal and athermal components [3, 4].

On the other hand, in the diffusion-controlled recovery creep model, the applied stress has only an athermal component which is comparable to the internal stress. The internal stress can only be reduced with the aid of diffusion; consequently, this kind of creep cannot proceed unless the internal stress is reduced to the level of the applied stress by diffusion-controlled recovery of the dislocation substructure, that is, an incubation time follows a small stress decrement during creep [5–7]. The diffusion-controlled recovery creep is "athermal" in the sense that the applied stress corresponds to the barrier of the long-range obstacles. The internal stress is ascribed to the substructure produced by strain-hardening during the primary creep stage [8].

Oytana *et al.* [9] have produced a rheological analysis of stress-drop tests based on different strain-hardening processes. According to their work, the substructure could be divided into two or more parts and, therefore, the internal stress should be composed of different components. Orlova and Cadek [10] pointed out that the internal stress is contributed to from two independent sources: the dislocation density within subgrains and the long-range stress field of subboundaries.

It is, therefore, important to interpret the high-temperature creep behaviour particularly in terms of the composition of the internal stress when the diffusion-controlled recovery creep is dominant. The purpose of this paper is to understand the steady state creep of a 25 wt % Cr–20 wt % Ni austenitic stainless steel from this point of view.

2. Experimental procedure

The chemical composition of the vacuum-melted austenitic stainless steel used in this study is

TABLE I Chemical compositions (wt %) of the vacuum-melted stainless steel without precipitates.

Cr	Ni	C	Mn	Si	S	P
22.77	21.39	0.005	Nil	0.02	0.009	0.004

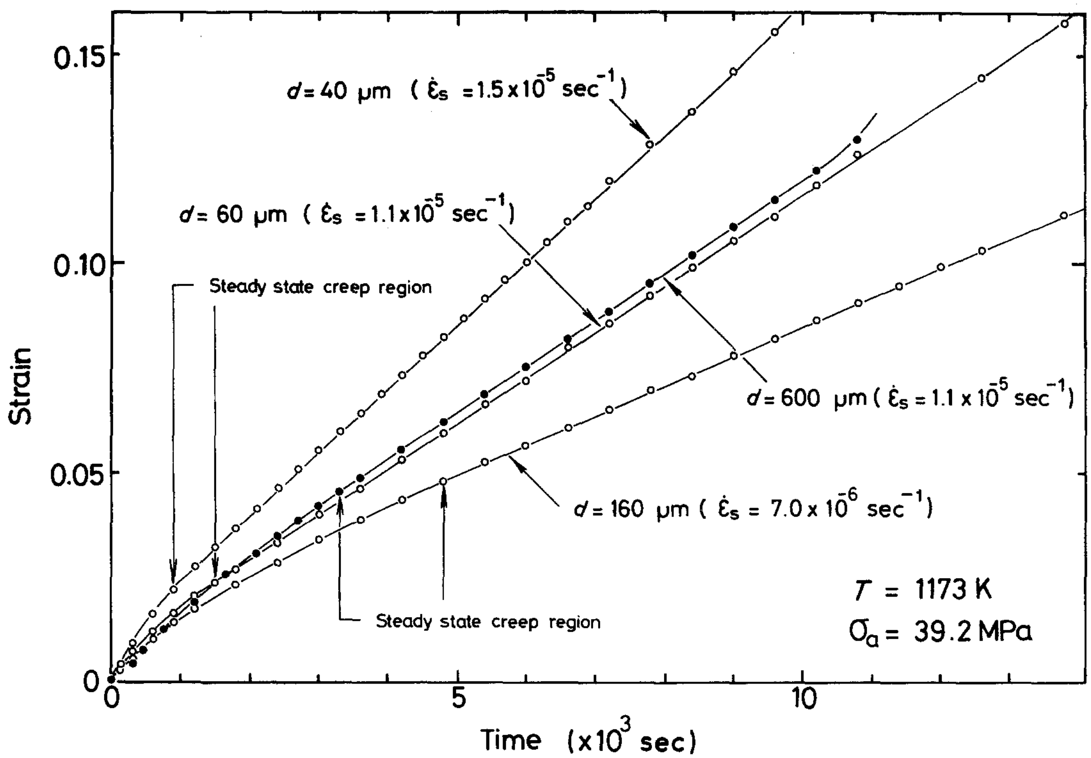

Figure 1 Creep cruves for specimens with diverse average grain diameters, *d*.

shown in Table I. This material has no precipitates. Specimens of diameter 2.0 mm and gauge length 40 mm were prepared as detailed in previous work [11, 12]. The mean grain diameter, d, was measured in each case by the grain intercept method.

Conventional creep tests were carried out in air after heating for 1 h at the test temperature, T. The test temperature range was 1133 to 1193 K, the stress range 9.8 to 39.2 MPa, and the grain size was found to range between 30 and 600 μm. The creep tests for samples with $d = 30\,\mu$m were performed only at $T \leqslant 1173$ K.

Stress-drop tests were performed in the steady-state creep region which had previously been ascertained by conventional creep tests [12]. The strain was measured to an accuracy of $\pm 0.5\,\mu$m using precision- and standard-dial gauges.

Creep stresses and creep strain rates were defined as follows:

σ_a is the creep stress in a conventional creep test without stress decrements;

σ_A is the initial applied stress in stress-drop tests;

$(\sigma_A - \Delta\sigma)$ is the applied stress after a stress decrement, $\Delta\sigma$;

$\dot{\epsilon}_s$ is the steady-state creep rate in a conventional creep test;

$\dot{\epsilon}_s$ is the creep rate in a new steady-state creep region reached after stress decrement from σ_A to $(\sigma_A - \Delta\sigma)$.

3. Experimental results

3.1. Steady state creep rates, $\dot{\epsilon}_s$, depending on grain size, d

Creep curves for $19.6\,\text{MPa} < \sigma_a \leqslant 39.2\,\text{MPa}$ are normal and independent of grain size, but the strain required to reach the steady-state creep region is dependent on the grain size, d, (Fig. 1). Figs 2–5 show the grain-size dependence of $\dot{\epsilon}_s$. It has been reported in previous work [11] that it is only for values of $d \leqslant 50\,\mu$m and values of $\sigma_a \leqslant 9.8$ MPa that $\dot{\epsilon}_s$ results from a vacancy creep along grain boundaries. The stress condition of $\sigma_a \geqslant 19.6$ MPa will make a power-law creep, $\dot{\epsilon}_s = A\sigma_a^n$, with $n = 4$–7, where A is a constant if T and d are constant [12]. For $d < 80\,\mu$m and $\sigma_a \geqslant 24.5$ MPa, the grain-size exponent, p, of $\dot{\epsilon}_s$ is nearly equal to minus one, if it is assumed that $\dot{\epsilon}_s \propto d^p$. This suggests that grain boundaries help

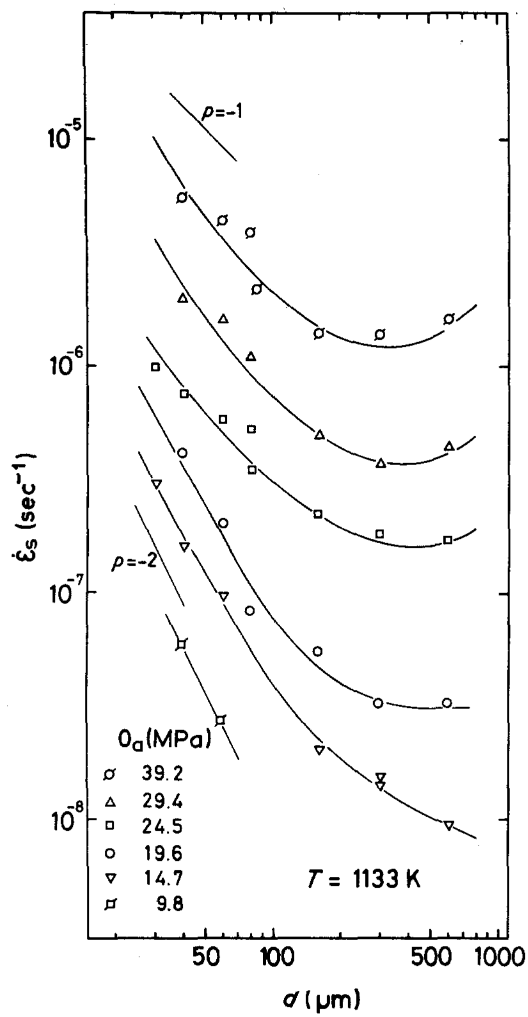

Figure 2 Grain-size dependence of $\dot{\epsilon}_s$ at a temperature of 1133 K.

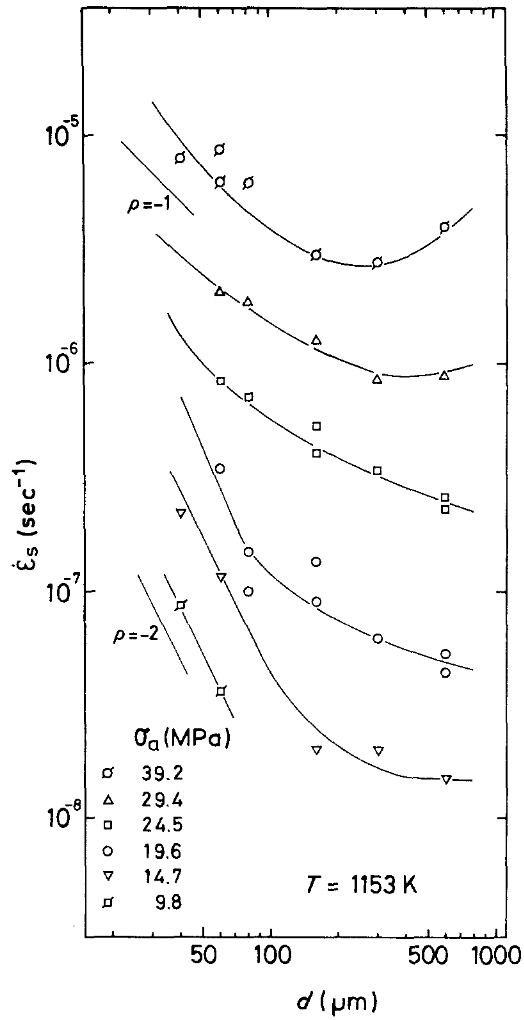

Figure 3 Grain-size dependence of $\dot{\epsilon}_s$ at a temperature of 1153 K.

the creep deformation, for $d < 80\,\mu$m and $\sigma_a \geqslant 24.5$ MPa, perhaps as sources and sinks of mobile dislocations [13]. In the medium- and coarse-grained specimens ($d \geqslant 80\,\mu$m), it is indicated that the dislocation-substructure has an influence on $\dot{\epsilon}_s$ [13, 14].

3.2. Stress-drop tests

Examples of strain–time relationships of stress-drop tests are shown in Fig. 6. There always exists an incubation time, Δt_i, even after the smallest stress decrement (1.56 MPa); then creep resumes and reaches a new steady-state creep stage at which the creep rate is $\dot{e}_s$. It is suggested that it is necessary for the level of the applied stress to be higher than or equal to the barrier of the long-range obstacles, in order to continue the creep deformation, i.e. it is necessary that the internal stress, σ_i, is close to σ_a. The creep in this study is in fact "athermal" (the diffusion-controlled recovery creep).

Incubation time, Δt_i, is plotted as a function of stress decrement, $\Delta\sigma$, in Fig. 7. There are critical values of $\Delta\sigma_c$, particularly in the medium- and coarse-grained specimens. For $\Delta\sigma \geqslant \Delta\sigma_c$, Δt_i increases very rapidly with increasing $\Delta\sigma$. If $\Delta\sigma$ is slightly larger (about 3–7 MPa) than $\Delta\sigma_c$, negative creep follows the stress drop, but the negative creep period is much shorter than Δt_i, as seen in Fig. 6.

$\sigma_A - \Delta\sigma_c$ has been defined as the strain-arrest stress, σ_c, in a previous work [12]. The existence of $\Delta\sigma_c$ indicates that the internal stress has a component which is easy to reduce. This is, hence-

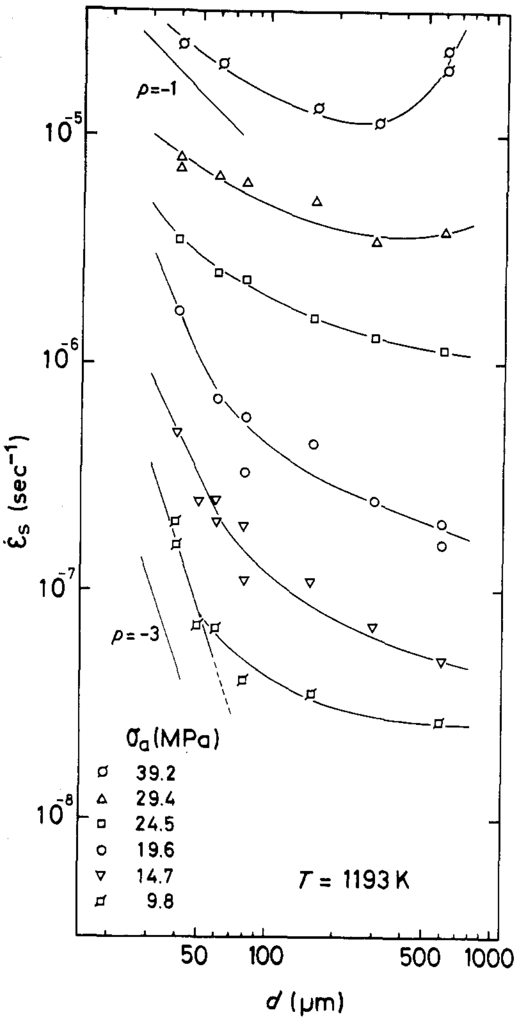

Figure 4 Grain-size dependence of $\dot{\epsilon}_s$ at a temperature of 1173K.

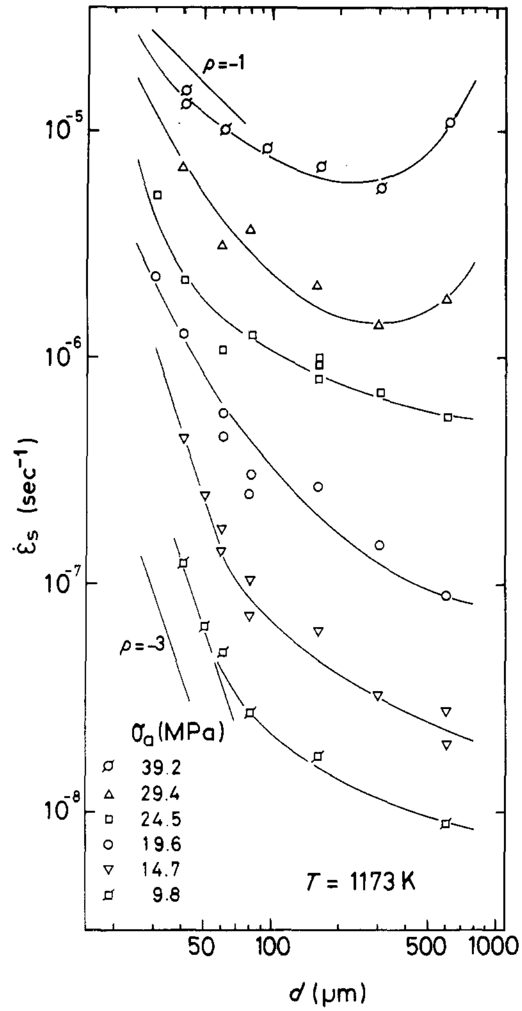

Figure 5 Grain-size dependence of $\dot{\epsilon}_s$ at a temperature of 1193K.

forth, referred to as the σ_s-component. So the internal stress, σ_i, has two independent components: σ_s and σ_c. It is considered that the σ_c-component expresses the background stress-field which is attributed to the metastable substructure [12].

Figs 8 and 9 show, respectively, the variation of σ_c with d and σ_a. σ_c does not depend only on the applied stress but also on the grain size. σ_c decreases with decreasing σ_a, and, if extrapolated, σ_c is equivalent to σ_a ($= \sigma_0$) at $\sigma_a = 5$–10 MPa. σ_0 will be discussed in Section 4.2. In the fine-grained specimens, it is difficult to estimate σ_c because the curves of $\Delta t_i = f(\Delta\sigma)$, where $f(\Delta\sigma)$ is a function of $\Delta\sigma$, for $d < 80\,\mu m$ have no obvious values of $\Delta\sigma_c$. It is suggested that the creep behaviour for $d < 80\,\mu m$ is essentially different from that of $d \geqslant 80\,\mu m$.

3.3. Steady-state creep rates, $\dot{e}_s$, after stress decrement

Figs 10–13 show the grain-size dependence of $\dot{e}_s$, which is compared with that of $\dot{\epsilon}_s$ under the same stress levels ($\sigma_a = \sigma_A - \Delta\sigma$). When $d < 80\,\mu m$, $\dot{e}_s$ is nearly equal to $\dot{\epsilon}_s$, whereas, for $80\,\mu m < d < 600\,\mu m$, $\dot{e}_s$ is less than $\dot{\epsilon}_s$. The difference between $\dot{e}_s$ and $\dot{\epsilon}_s$ increases with increasing initial applied stress, σ_A, as indicated in these figures. The fact that $\dot{e}_s < \dot{\epsilon}_s$ for $80\,\mu m < d < 600\,\mu m$ suggests that a part of the substructure produced during creep under σ_A can remain metastable, even in a new quasi-steady-state creep stage after stress reduc-

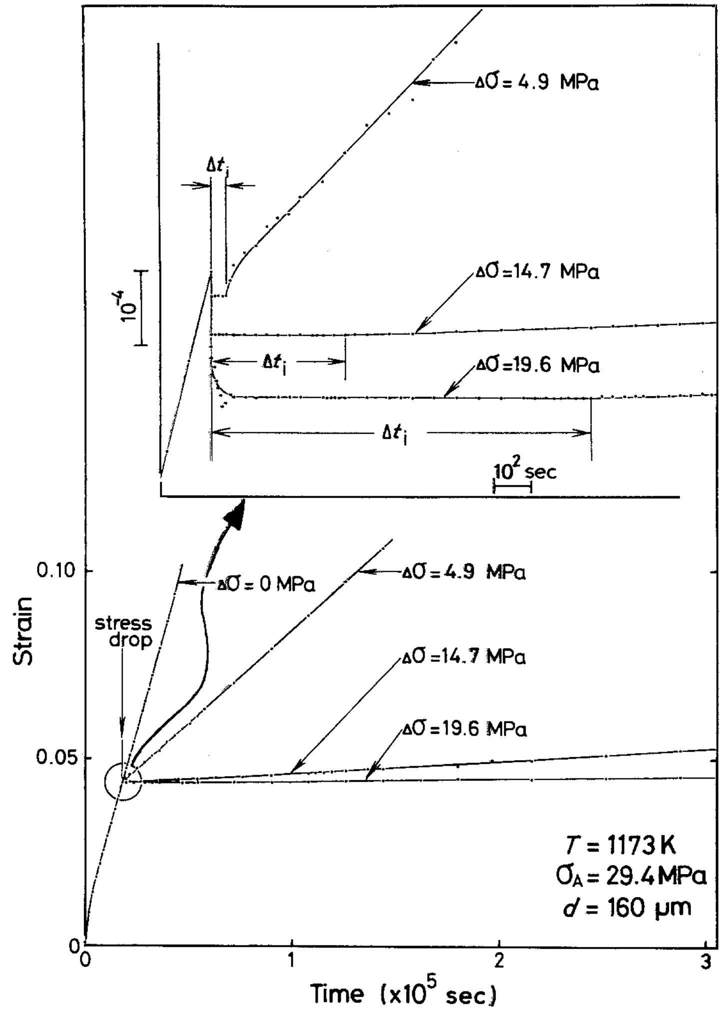

Figure 6 Strain–time relationships in stress-drop experiments. The inset shows the region of the stress-drop in more detail.

tion. The internal stress in the new steady-state creep stage is different in composition from that in the general steady-state creep region at the reduced stress level ($\sigma_a = \sigma_A - \Delta\sigma$).

3.4. Recovery rate

The recovery rate, r, during creep is given by the following equation [15–17]

$$r = \left.\frac{\Delta\sigma}{\Delta t_i}\right|_{\Delta\sigma\to 0}. \qquad (1)$$

Figs 14 and 15 show the recovery rates, r, as functions of σ_a and $\sigma_a - \sigma_c$, respectively. r as a function of $\sigma_a - \sigma_c$ ($= \sigma_i - \sigma_c = \sigma_s$) makes the stress exponents, n^*, approximately equal to three, which is predicted by the growth of the overall average mesh size of the three-dimensional dislocation networks with sub-grains [16, 18]. It should, however, be noted that the incubation time for $\Delta\sigma < \sigma_s$ and r is not always attributed to such growth as stated in the literature [7, 17], although $\sigma_a - \sigma_c$ ($= \sigma_s$) must play an important part in the creep deformation.

3.5. $\dot{\epsilon}_s$ as a function of σ_s

Fig. 16 shows the steady-state creep rates, $\dot{\epsilon}_s$, which are re-arranged under the same condition of $\sigma_s = \sigma_a - \sigma_c = 15$ MPa. It is shown that the grain-size has no influence on $\dot{\epsilon}_s$ of a function of σ_s. It appears that the effect of grain boundaries on the creep for grain sizes, d, greater than 80 μm is taken into the strain-arrest stress as a part of the background obstacles, and that σ_s-component is, virtually, the driving stess for creep.

4. Discussion

In this study it was apparent that diffusion-controlled recovery creep is the dominant creep

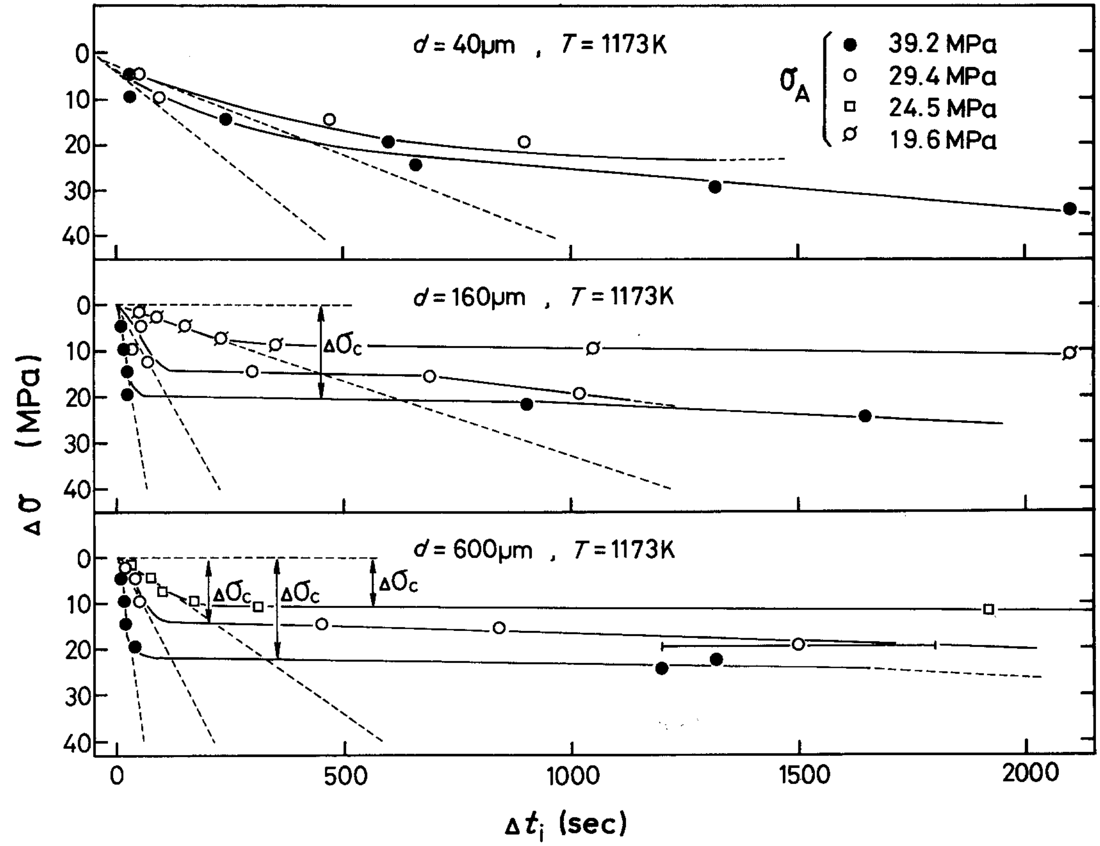

Figure 7 Plot of incubation time against stress decrement.

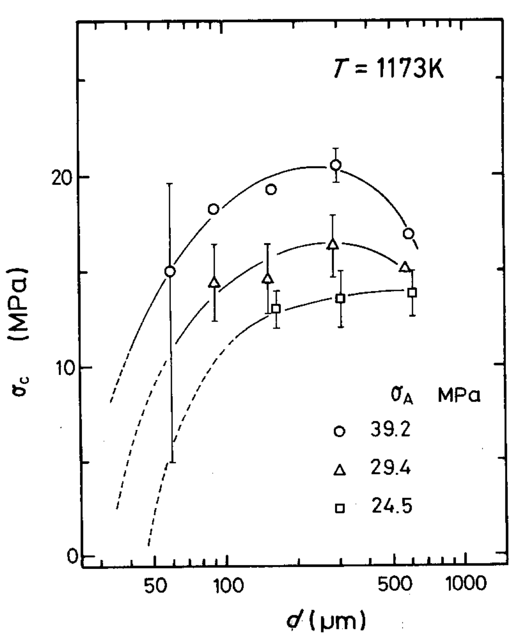

Figure 8 Variation of σ_c with grain size.

mechanism, i.e., the internal stress, σ_i, is comparable to the applied stress. It is considered that the internal stress is made up of two components: σ_c and σ_s, such that

$$\sigma_i = \sigma_c + \sigma_s, \tag{2}$$

where σ_c is the strain-arrest stress, owing to persistent long-range obstacles which cannot contribute to the creep deformation, and σ_s is a component which can be easily reduced with the help of diffusion. As above mentioned, σ_s is comparable to the driving stress for creep.

4.1. An explanation of the fact that $\dot{e}_s$ is less than $\dot{\varepsilon}_s$

Fig. 17 shows schematically the composition of σ_i, according to that variation of σ_c with σ_a shown in Fig. 9. A possible explanation for this behaviour may be as follows. When the applied stress is dropped from σ_1 to σ_2 on a specimen undergoing steady-state creep at $\sigma_a = \sigma_1$, the σ_c-component of

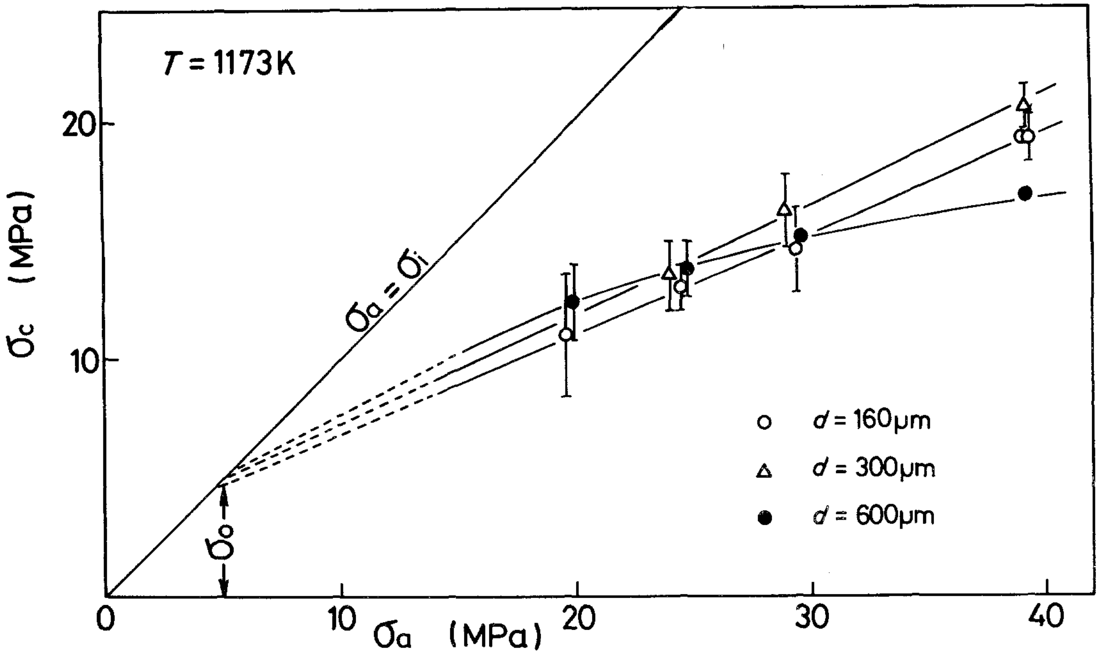

Figure 9 Variation of σ_c with applied stress (σ_a).

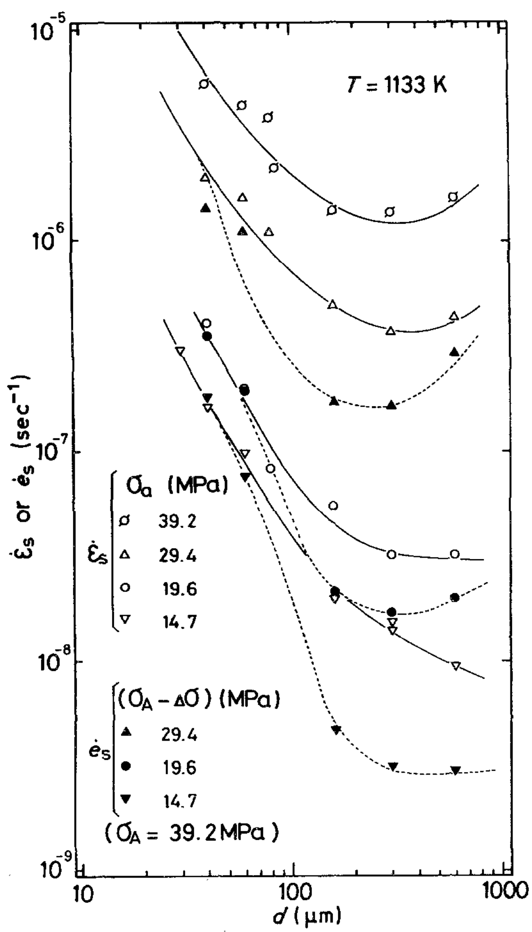

Figure 10 Grain-size dependence of $\dot{e}_s$ at a temperature of 1133 K and σ_A = 39.2 MPa.

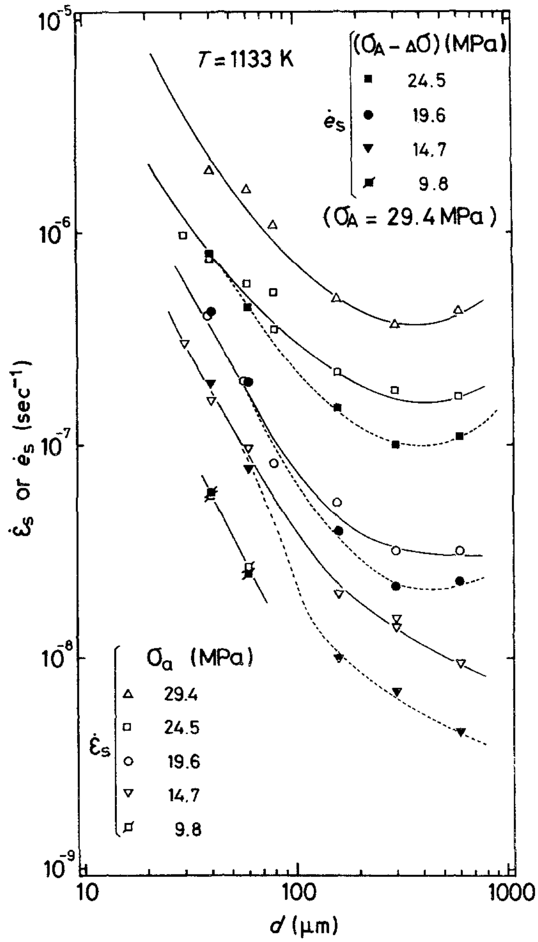

Figure 11 Grain-size dependence of $\dot{e}_s$ at a temperature of 1133 K and σ_A = 29.4 MPa.

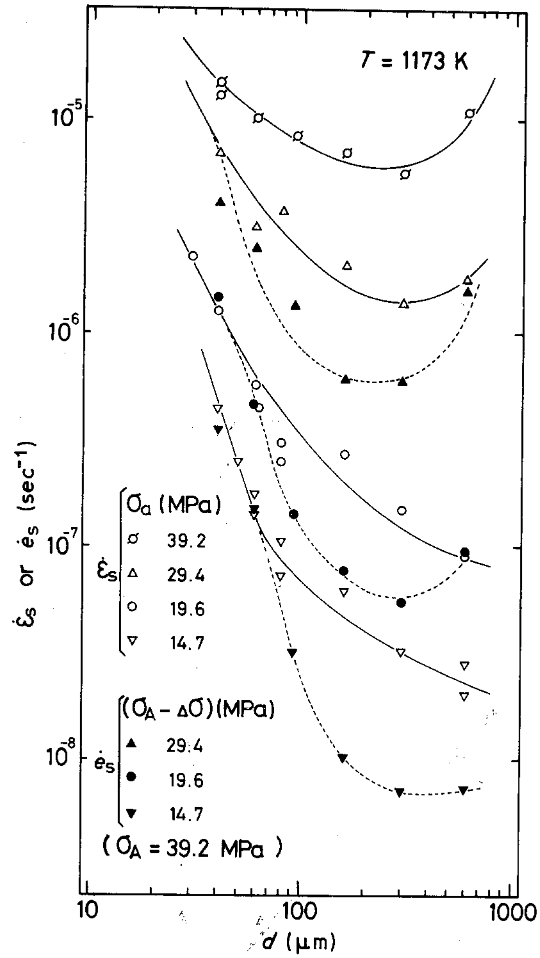

Figure 12 Grain-size dependence of $\dot{e}_s$ at a temperature of 1173 K and $\sigma_A = 39.2$ MPa.

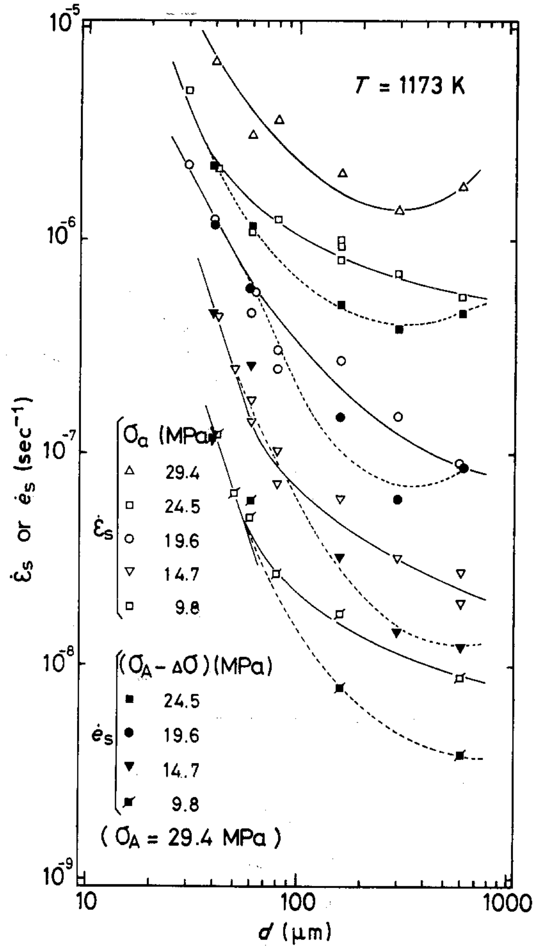

Figure 13 Grain-size dependence of $\dot{e}_s$ at a temperature of 1173 K and $\sigma_A = 29.4$ MPa.

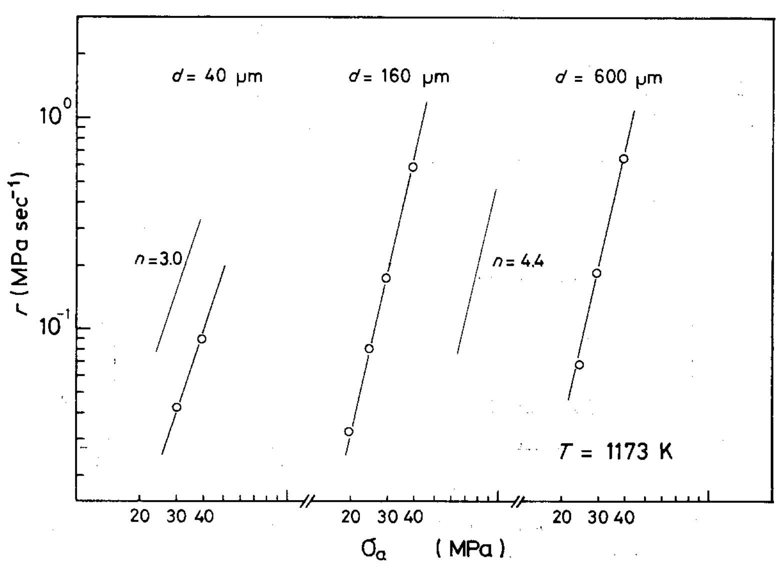

Figure 14 Variation of recovery rate, r, with σ_a. n is a stress exponent of r.

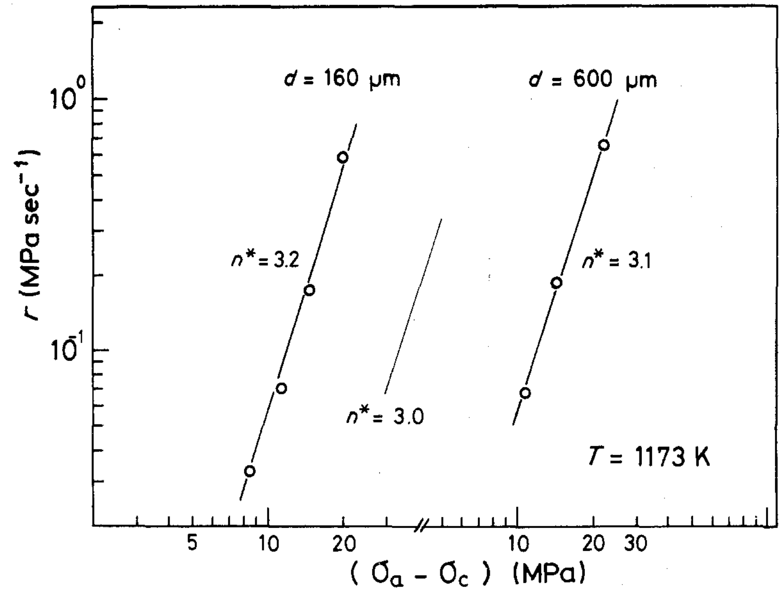

Figure 15 Variation of recovery rate with $\sigma_a - \sigma_c$.

σ_{c1} is not reduced to σ_{c2} but only to σ_{c3}, so that the σ_s-component results in $\sigma_2 - \sigma_{c3}$. As has been reported in a previous work [12], $\dot{\epsilon}_s \propto (\sigma_a - \sigma_c)^4 \approx \sigma_s^4$, and, except in the case of fine-grained specimens, $\dot{\epsilon}_s$ under $\sigma_a = \sigma_2$ is given by

$$\dot{\epsilon}_s = A_0(\sigma_2 - \sigma_{c2})^4, \quad (3)$$

where A_0 is a constant if T is constant.

On the other hand, $\dot{e}_s$, after stress reduction from σ_1 to σ_2, is expressed by

$$\dot{e}_s = A_0(\sigma_2 - \sigma_{c3})^4. \quad (4)$$

$\dot{e}_s$ is, therefore, less than $\dot{\epsilon}_s$, because $\sigma_{c2} < \sigma_{c3}$.

For the fine-grained specimens, $\dot{e}_s$ is nearly equal to $\dot{\epsilon}_s$. This indicates that $\sigma_{c2} \approx \sigma_{c3}$, or grain boundaries loose the persistency of σ_c.

4.2. On the existence of σ_0

In Fig. 17, if σ_2 is less than σ_{c1}, positive creep will not be produced until the σ_c-component is reduced to σ_2. In $\sigma_a \leqslant \sigma_0$, the internal stress has only the σ_c-component and no σ_s-component, so that the creep deformation mechanism disclosed in the present paper cannot make progress, although other creep mechanisms, for instance, viscous flow [1], vacancy creep [19, 20], or free grain-boundary sliding [21, 22] may take place. Fig. 13 indicates that $\sigma_0 = 5$–10 MPa at $T = 1173$ K. It has been reported in previous work [11] that, at temperatures around 1173 K, a discontinuous point appears at $\sigma_a = 5$–10 MPa on a log $\dot{\epsilon}_s$ against log σ_a plot for the medium- and coarse-grained specimens, and a vacancy creep by grain-boundary diffusion is produced at $\sigma_a \leqslant 9.8$ MPa and $d \leqslant 50\,\mu$m. It seems that the existence of σ_0 results in this behaviour.

σ_0 should not be thought of as evidence for the existence of a friction stress [5, 23], but only as the transition of creep deformation mechanism.

5. Conclusions

(a) The steady-state creep of a 25 wt % Cr–20 wt % Ni austenitic stainless steel is recovery-controlled over the stress range 9.8–39.2 MPa and the temperature range 1133–1193 K.

(b) The internal stress, σ_i, is close to the applied stress, and is expressed by Equation 2 i.e. $\sigma_i = \sigma_c + \sigma_s$, where σ_c is the strain-arrest stress due to

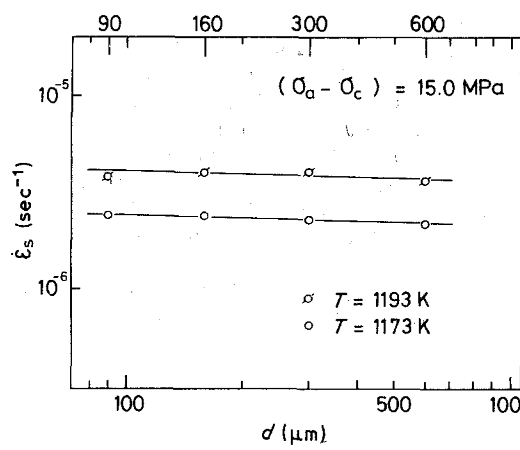

Figure 16 Grain-size dependence of $\dot{\epsilon}_s$ as a function of $\sigma_s = \sigma_a - \sigma_c$.

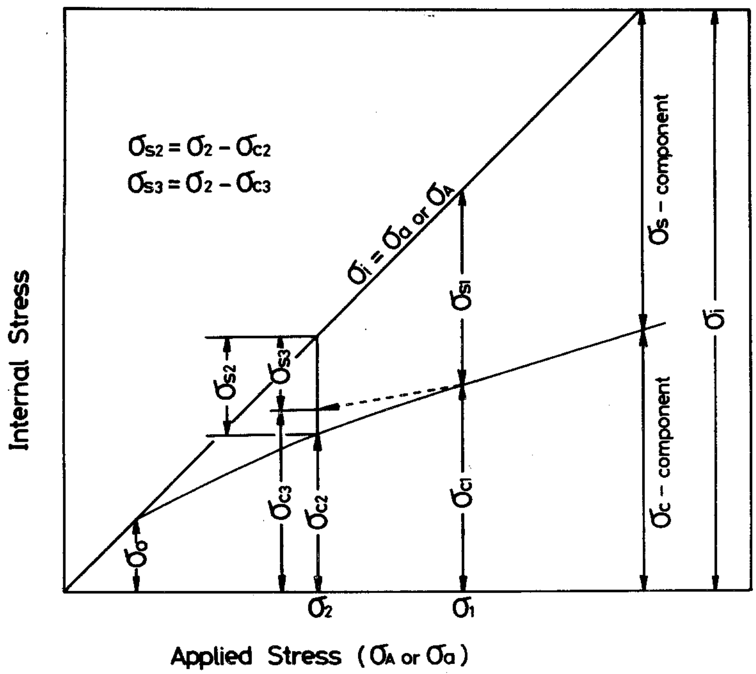

Figure 17 Schematic diagram of the composition of the internal stress.

persistent long-range obstacles (metastable substructure), and σ_s is a component possible to reduce easily and is comparable to the driving stress for creep.

(c) The steady state creep for $d \geqslant 80\,\mu\text{m}$ may be accounted for in terms of the composition of the internal stress.

(d) The steady state creep for $d < 80\,\mu\text{m}$ is dominantly controlled by grain boundaries.

(e) There exists a parameter, σ_0, so that, for $\sigma_a \leqslant \sigma_0$, the internal stress has only a σ_c-component. σ_0 means the transition of creep deformation mechanism.

References

1. J. P. POIRIER, *Acta Met.* **25** (1977) 913.
2. *Idem*, "Plasticité à Haute Température des Solides Cristallins (Eyrolles, Paris, 1976) p. 1.
3. H. CONRAD, *J. Metals* **16** (1964) 582.
4. *Idem, Mater. Sci. Eng.* **6** (1970) 265.
5. P. W. DAVIES, G. NELMAS, K. R. WILLIAMS and B. WILSHIRE, *Metals Sci.* **7** (1973) 87.
6. J. D. PARKER and B. WILSHIRE, *ibid.* **12** (1978) 453.
7. B. BERGMAN, *Scand. J. Metall.* **4** (1975) 109.
8. C. N. AHLQUIST and W. D. NIX, *Acta Met.* **19** (1971) 373.
9. C. OYTANA, P. DELOBELLE and A. MERMET, *J. Mater. Sci.* **14** (1979) 549.
10. A. ORLOVÁ and J. ČADEK, *Z. Metall.* **65** (1974) 55.
11. Y. TAKAHASHI and T. YAMANE, *J. Mater. Sci.* **14** (1979) 2818.
12. Y. TAKAHASHI, K. NAKAGAWA and T. YAMANE, *Z. Metall.* **71** (1980) 572.
13. F. GAROFALO, W. F. DOMIS and F. VON GEMMINGEN, *Trans. Met. AIME* **230** (1964) 1460.
14. O. D. SHERBY, *Acta Met.* **10** (1962) 135.
15. K. R. WILLIAMS and I. R. MCLAUCHLIN, *J. Mater. Sci.* **5** (1970) 1063.
16. H. E. EVANS and G. KNOWLES, *Acta Met.* **25** (1977) 963.
17. J. B. BILDE-SØRENSEN, *Phil. Mag.* **38** (1978) 1.
18. B. BURTON, *Metals Sci.* **9** (1975) 297.
19. H. OIKAWA and S. KARASHIMA, *Jap. Inst. Metals* **11** (1972) 567.
20. M. F. ASHBY, *Acta Met.* **20** (1972) 887.
21. F. W. CROSSMAN and M. F. ASHBY, *ibid.* **23** (1975) 425.
22. R. C. GIFKINS, *Metal Trans.* **7A** (1976) 1225.
23. W. R. THORPE and I. O. SMITH, *Phil. Mag. A* **40** (1979) 581.

Received 29 May and accepted 8 July 1980.